UNIVERSITY OF BIRMINGHAM

The Role of Persulfides and ALDH2 in Myocardial Ischaemia-Reperfusion Injury.

Year 3

BSc Biomedical Science

ID #2158143

April 2023

Table of contents

Abbreviations **III**
Abstract **V**
1. Introduction **1**
1.1 Pathophysiology of acute myocardial infarction 2
1.2 Pathophysiology of myocardial ischaemia-reperfusion injury 3
1.3 The role of ALDH2 following myocardial IRI 5
1.4 The role of NO following myocardial IRI 6
1.4.1 Physiology of NO 6
1.4.2 Oxidative stress and hydropersulfides 9
1.4.3 Cardiovascular endothelium and NO pathways 10
1.5 PKG 1α oxidation and the heart 11
1.5.1 PKG 1α physiology and functions 11
1.5.2 PKG 1α oxidation 11
1.6 Summary 13
1.7 Hypothesis 13
1.8 Aims 14
2. Materials and methods **14**
2.1 Genotyping of ALDH2 mice 15
2.2 Langendorff protocol 18
2.2.1 Assessment of infarct size 20
2.3 Western blotting for PKG 1α oxidation 22
2.3.1 Dimerization protocol for PKG 1α oxidation 22
2.3.2 Western blotting 22
2.3.3 Analysis of blots 27
2.4 Statistical analysis 27
3. Results **28**
3.1 Cysteine trisulfide reduces infarct size following IRI in ALDH2 deficient mice 28
3.2 Increased PKG 1α oxidation in ALDH2 deficient mice following myocardial IRI 30
4. Discussion **32**
4.1 Elucidation of the role and mechanism of cysteine trisulfide in protection against IRI 32
4.2 The role of ALDH2 in PKG 1α oxidation and its efficacy for protection against IRI 38
4.3 Summary 41
5. References **42**

Abbreviations

IRI	Ischaemia-reperfusion injury
ALDH2	Aldehyde dehydrogenase 2
PKG 1α	Protein kinase-G 1α
cys-SSS-cys	Cysteine trisulfide
cysSSH	Cysteine persulfide
CAD	Coronary artery disease
AMI	Acute myocardial infarction
STEMI	ST elevation acute myocardial infarction
NSTEMI	non-ST elevation acute myocardial infarction
PCI	Percutaneous coronary intervention
ATP	Adenosine triphosphate
ROS	Reactive oxygen species
MDA	Malondialdehyde
4-HNE	4-hydroxynonenal
SGLT2i	Sodium glucose cotransporter 2 inhibitors
NLRP3	Nucleotide binding oligomerization domain-like receptor protein 3
AMPK	AMP-activated protein kinase
Akt	Protein kinase B
mTOR	Mammalian target of rapamycin
NO	Nitric oxide
NOS	Nitric oxide synthase
eNOS	Endothelial nitric oxide synthase
EDRF	Endothelium derived relaxing factor
EDHF	Endothelium derived hyperpolarizing factor
H_2S	Hydrogen sulfide
sGC	Soluble guanylyl cyclase
cGMP	Cyclic guanosine monophosphate
BH4	Tetrahydrobiopterin
kDa	Kilodalton
TRPC6	Transient receptor potential channel 6
Cn/NFAT	Calcineurin/nuclear factor of activated T cells
WT	Wild type
KO	Knock-out
KI	Knock-in
HET	Heterozygous
PCR	Polymerase chain reaction
KHB	Krebs-Henseleit buffer
KCL	Potassium chloride

Kh2po4	Monobasic potassium phosphate
Nahco3	Sodium bicarbonate
Mgso4	Magnesium sulfate
CacI2	Calcium chloride
TTC	Triphenyltetrazolium chloride
TEMED	Tetramethylethylenediamine
APS	Ammonium sulfate
ddH_2O	Double distilled water
SDS	Sodium dodecyl sulfate
PVDF	Polyvinylidene difluride
BSA	Bovine serum albumin
PBS	Phosphate-buffered saline
LKB1	Liver kinase B1
PTEN	Phosphate and tensin homolog
SHR-SP	Stroke-prone spontaneously hypertensive rats
PKCε	Protein kinase C epsilon type
CARS	Cysteinyl-tRNA synthetase
GKAP	G-kinase anchoring proteins

Abstract

Restoring blood flow following an acute myocardial infarction (AMI) can lead to ischaemia-reperfusion injury (IRI). IRI involves cell membrane damage and tissue death, therefore finding a novel therapeutic intervention is imperative to protect the heart from significant injury and subsequent failure. Specifically, investigation of aldehyde dehydrogenase 2 (ALDH2), protein kinase-G 1α (PKG 1α) and cysteine trisulfide (cys-SSS-cys) is key as they have shown significant potential as cardioprotective agents. This study aimed to investigate the effects of ALDH2 deficiency on infarct size and PKG 1α oxidation following IRI, as well as the effects of cys-SSS-cys on infarct size following IRI. To determine the impact of cys-SSS-cys and ALDH2 deficiency our investigation utilised a well-established Langendorff model to assess infarct size and PKG 1α oxidation. We here demonstrate that cys-SSS-cys improves myocardial recovery following ischaemia-reperfusion by reducing infarct size. In addition, 2 hours of reperfusion leads to a significant increase in PKG 1α oxidation. Further investigation is warranted to dissect the mechanism of cys-SSS-cys and other potential cardioprotective agents. As well as this, further investigation of the efficacy of PKG 1α oxidation will help to inform the next steps for its involvement in potential therapeutic strategies.

1. Introduction

Coronary artery disease (CAD), which encompasses acute myocardial infarction (AMI) and stroke, remains responsible for the greatest number of single cause mortalities worldwide, with 18.56 million people dying in 2019 from cardiovascular diseases alone (figure 1.1). (1) The main cause of CAD is atherosclerosis, which is the build-up of fatty deposits, cholesterol or other molecules on the artery wall. This tiny change leads to a whole cascade of small events which then compound to have a devastating effect. The build up of this plaque leads to a narrowing of the blood vessels responsible for providing oxygen to the heart, also causing lesions which reduce blood vessel diameter further. On occasion, bursting of plaques can lead to a blood clot, which severely minimises perfusion to the heart. (2) Risk factors of CAD include, but are not limited to, smoking, obesity, genetics, diabetes and hypertension. (2) Current methods for the management of CAD mainly include lifestyle changes such as quitting smoking or having a more balanced diet, with the goal being an improvement of cardiovascular health alongside the prevention of AMI and stroke. Despite the prevalence of recent research and the growing capabilities of technology, mortality rates and incidence of CAD continues to rise due to increasing obesity rates and an ageing population. (2) Therefore, more research is required to understand the mechanisms of CAD and identify potential therapeutic targets.

Treatment of CAD is similar to its management, however in conjunction with this there are several medications that can be taken, such as aspirin, statins, beta-blockers, and calcium

channel blockers. In some more severe cases, invasive treatment includes the insertion of a coronary artery stent or coronary artery bypass surgery. (3)

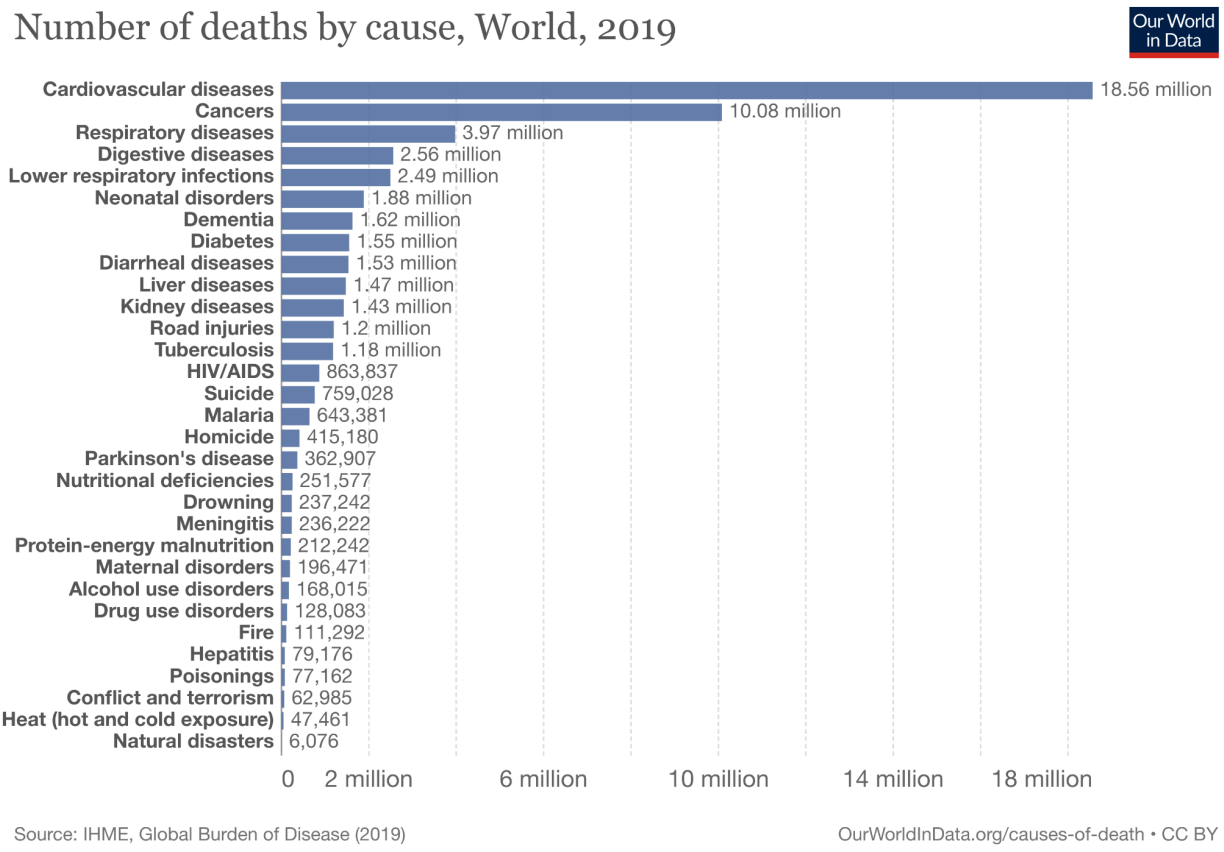

Figure 1.1 *Graphical representation of global cardiovascular disease mortality rates. Cardiovascular disease had the largest single cause mortality rate globally in 2019 (18.56 million), roughly 8 million greater than cancer (10.08 million), and almost 15 million greater than respiratory diseases (3.97 million) the third largest single cause of death globally in 2019. (1)*

1.1 Pathophysiology of acute myocardial infarction

AMI is one of the subsequent events that can be caused by CAD and occurs when there is a decrease or complete loss of blood flow and oxygen supply to the coronary artery, disrupting the myocardium. (4) Death of cardiomyocytes can be verified through tests for the cardiac protein biomarker troponin. (5) ST elevation AMI (STEMI) occurs due to complete occlusion of

the coronary artery due to rupture of plaque and thrombus. In contrast, non-ST elevation AMI (NSTEMI) occurs due to coronary spasms and other factors that restrict blood flow. STEMI patients are generally treated with percutaneous coronary intervention (PCI), which involves opening the arteries, often with a stent. Another option is thrombolysis, which involves the breakdown of blood clots through medication such as alteplase. (6) Whereas treatment for patients with NSTEMI usually involves blood thinning medication, such as heparin or warfarin. Speed of treatment in reaction to a suspected AMI is vitally important for the chances of the patient's survival. (7)

1.2 Pathophysiology of myocardial ischaemia-reperfusion injury

Following an AMI, blood supply to the occluded zone must be rapidly restored, especially for the survival of the myocardium. However, IRI can occur when this process has a paradoxical effect, leading to further damage and sometimes death to the cardiomyocytes. (8)

Ischaemia is detected when the oxygen supply, as well as other nutrients like glucose, do not meet the body's demand. Alterations in metabolic function begin, leading to a lack of adenosine triphosphate (ATP) production, and ionic imbalance. Phospholipases start to degrade membrane lipids in ischaemic conditions leading to disruption in cell membrane integrity and increased levels of fatty acids circulating the body. (8) Reactive oxygen species (ROS) play a key role in IRI. Major ROS production includes superoxide anion, hydrogen peroxide and hydroxyl radical. Upon reperfusion of ischaemic tissue, uric acid is produced which leads to the conversion of superoxide anion to hydrogen peroxide and the hydroxyl radical. The hydroxyl radical causes lipid peroxidation, which is a metabolic process that

induces a chain reaction involving oxidation of lipids to form a lipid radical, then a lipid peroxyl radical, which gives rise to a lipid peroxide (figure 1.2). (8) End products of lipid peroxidation include reactive aldehydes such as malondialdehyde (MDA) and 4-hydroxynonenal (4-HNE). If lipid peroxidation is not halted, this will subsequently lead to cell membrane damage and eventually death of cardiomyocytes. (8) Second to this, a study by Marnett et al, found that these end products of lipid peroxidation may have mutagenic and carcinogenic effects. (9)

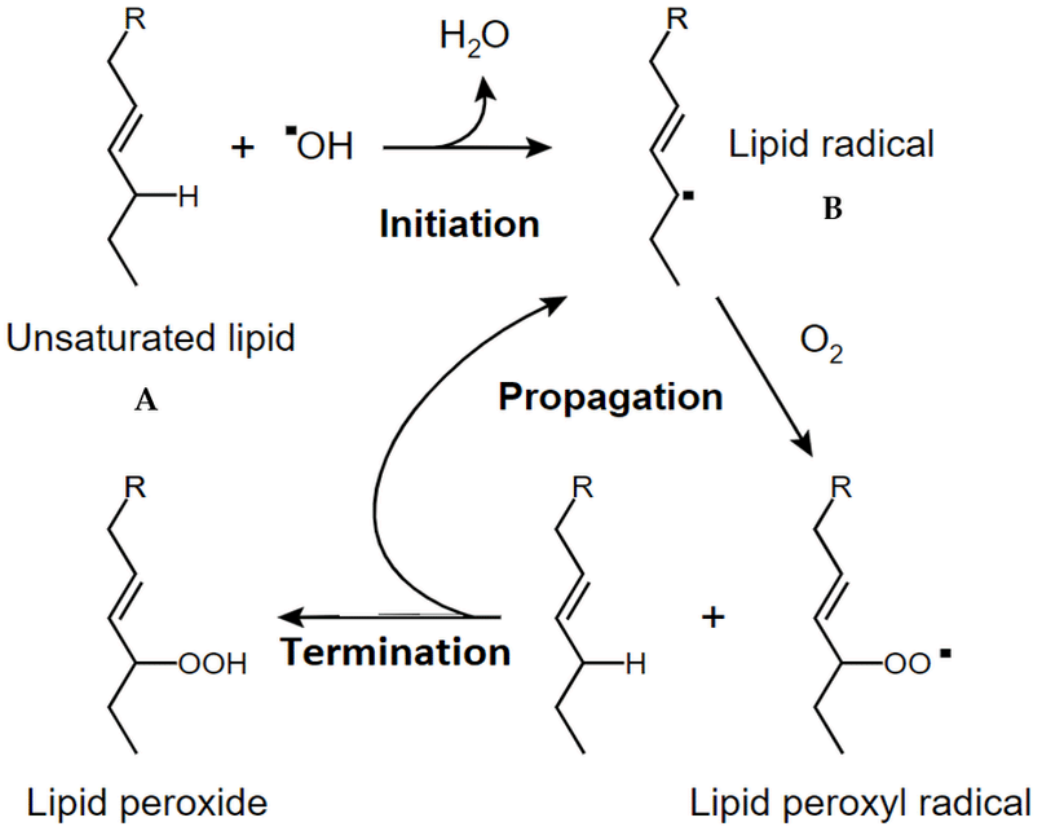

Figure 1.2. *Stages of lipid peroxidation.* ***1.*** *Oxidation of an unsaturated lipid produces a lipid radical.* ***2.*** *The lipid radical reacts quickly with oxygen to form a lipid peroxyl radical.* ***3.*** *The lipid peroxyl radical attracts a hydrogen atom from another lipid molecule, producing another lipid radical, and a lipid peroxide. Production of another lipid radical causes the chain to become cyclical. This chain of reactions will continue until antioxidants are produced to terminate lipid peroxidation. (10)*

1.3 The role of ALDH2 following myocardial IRI

An important mitochondrial enzyme in the aftermath of AMI and IRI is the ALDH2 enzyme, encoded by the ALDH2 gene, on chromosome 12. (11) ALDH2's main function is in the oxidation pathway of the metabolism of alcohol, however, it has also been found to protect against oxidative stress. In 2006, Ohta et al found that ALDH2 deficient cells were highly vulnerable to 4-HNE, one of the main products of lipid peroxidation. Synchronously these cells were also sensitive to antimycin A-induced oxidative stress, as well as the build-up of proteins modified by 4-HNE. (12) More recent studies have shown that ALDH2 provides cardioprotection through its ability to directly break down 4-HNE. Approximately 560 million people in East-Asian countries have an ALDH2 deficient genotype, causing flushing-like symptoms commonly associated with alcohol due to an inability to break down acetaldehyde. This mechanism results in several cardiovascular conditions associated with ALDH2 deficiency due to the toxicity of some acetaldehydes like 4-HNE. (13) Most recently in 2023, a new study by Guo et al, found that sodium glucose cotransporter 2 inhibitors (SGLT2i) reduced endothelial dysfunction associated with this ALDH2 deficient genotype. (14) Nitroglycerin tolerance leads to an increase in cardiac dysfunction, but this can be counteracted with an ALDH2 activator, which leads to a decrease in infarction size upon injury. (15) Overexpression of ALDH2 has been found to reduce cardiotoxicity by decreasing ROS production. This reduces inflammation and cell pyroptosis caused by activation of nucleotide binding oligomerization domain-like receptor protein 3 (NLRP3). (16) A 2010 study by Zhang et al, found that ALDH2 protects against IRI not only through detoxifying acetaldehydes but also through alternate regulation of autophagy controlled by AMPK-mTOR and Akt-mTOR signalling cascades. (17) Results showed that ischaemia-induced AMPK

activation was enhanced by ALDH2 overexpressing hearts, compared to a decrease in activation in ALDH2 knockout hearts. Similarly, reperfusion-induced activation of Akt was also enhanced by ALDH2 overexpressing hearts and decreased by ALDH2 knockout hearts. (17)

1.4 The role of NO following myocardial IRI

1.4.1 Physiology of NO

Endogenously produced from L-arginine by the nitric oxide synthase (NOS) enzyme, NO is a highly reactive free radical molecule with variable, tissue specific functions. It is also an endothelium-derived relaxing factor (EDRF) and can be produced from the reduction of inorganic nitrates. (18) NO plays a vital role in the cardiovascular system for preventing the onset or progression of cardiovascular disease. Regulation of blood pressure, prevention of platelet aggregation, and inhibition of smooth muscle proliferation are all key cardioprotective functions of NO. (18) NO is produced in endothelial cells alongside hydrogen sulfide (H_2S), which contributes to the regulation of vasodilation and angiogenesis. (19) During physiological conditions and/or normoxia, NO works to maintain cardiovascular homeostasis through a pathway involving the NO receptor soluble guanylyl cyclase (sGC), and cyclic guanosine monophosphate (cGMP), known as the NO-sGC-cGMP pathway. cGMP provides vasodilatory effects, facilitating blood and oxygen supply. cGMP activates protein kinase G (PKG), leading to smooth muscle relaxation, platelet inhibition and changes in gene expression (figure 1.3). (20) Dysfunction of this pathway can be seen during ischaemia, however, recent studies have found that there is an alternative pathway available for NO production. This is known as the “nitrate-nitrite-NO pathway”, which is believed to improve endothelial function, thus helping to

maintain cardiovascular homeostasis and protect against atherogenesis and IRI. (20) This discovery has led to many studies investigating the relevance of dietary nitrate supplementation for the maintenance of improved cardiovascular health. (20) This includes not only hypertensive and CAD patients, but also many healthy individuals such as athletes, looking for a competitive edge which may be found in the efficiency of their cardiovascular system. (21-23) Approximately 25% of dietary nitrates from green leafy vegetables and cured meat are reduced to nitrite in the mouth, via the enzyme nitrate reductase. (24) Nitrite is then reduced to NO in the stomach via acidosis and/or nitrate reductases (e.g. transmembrane and periplasmic reductases), (25) and any excess nitrites enter the bloodstream where they are reduced to NO in ischaemic conditions. (26) NO subsequently improves mitochondrial efficiency as well as blood flow. (20)

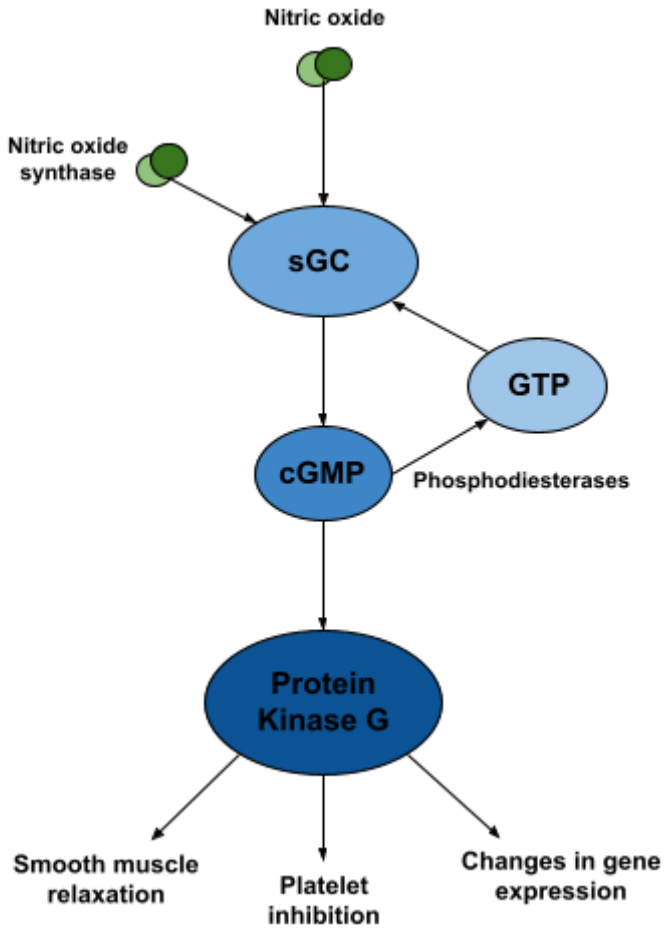

Figure 1.3. *Diagram outlining normoxic NO pathway - adapted from reading.ac.uk (27)*

In the first 15 minutes of ischaemia, there is an increase in NO levels through activation of endothelial nitric oxide synthase (eNOS) enzyme. (8) A previous study by Köken et al, demonstrated this in rat liver tissue. (28) During early reperfusion a decline in NO levels can be seen due to loss of endothelial and eNOS function, as well as increased production of ROS. (8) Lower eNOS levels can increase the risk of vasoconstriction, a common effect seen in rat models during ischaemia-reperfusion. (28) As mentioned, the pathology of NO is

variable, as NO has oxidant and antioxidant properties, with NO shown to be inactivated by superoxide anion to stimulate lipid peroxidation. (29) Cardiovascular IRI is well researched, with results showing NO provides a cardioprotective effect, but conversely, NO may lead to harmful effects such as cytotoxicity during skeletal IRI. (30) NO has an unpaired electron in its outer ring, giving it antioxidant tendencies, such as reducing other molecules, which supports the proposed mechanism of its ability to inhibit lipid peroxidation. As mentioned, the reason high doses have seen harmful effects is because NO is inactivated by superoxide anion to form peroxynitrite, a highly efficacious oxidant. (30) This indirect mechanism gives the appearance of NO directly contributing to the harmful effects of IRI. The balance between NO and superoxide anion is vitally important in our knowledge and ability to control lipid peroxidation. Control of this balance may also see other benefits away from IRI, to do with oxidative stress such as reduced atherosclerosis. (31)

1.4.2 Oxidative stress and hydropersulfides

Oxidative stress occurs when there is a shift in the balance between ROS production and the body's ability to detoxify these molecules, leading to cellular damage. Hydropersulfides are key antioxidants, helping to protect cells from oxidative stress. A recent study by Barayeu et al, showed that hydropersulfides inhibit ferroptosis, a type of cell death driven by lipid peroxidation. (32) This type of sulfane species can effectively detoxify free radicals, thereby limiting lipid peroxidation. The study shows that hydropersulfides may be able to prevent radical chain reactions through the formation of perthiyl radicals. Additionally, hydropersulfides can undergo autocatalytic regeneration, which means that low concentrations are sufficient to provide protective effects. (32) One particular species that has been shown to protect against myocardial IRI, is cysteine persulfide (cysSSH). A recent study by Griffiths et al, (33)

demonstrated that endogenous cysSSH concentrations are increased during ischaemia and are returned to base levels at the start of reperfusion. (33) Exogenous administration of cysteine trisulfide (cys-SSS-cys), a cysSSH donor, can help to keep cysSSH concentrations high during reperfusion, which led to decreased MDA and 4-HNE concentrations, the undesirable end products of lipid peroxidation mentioned previously. cys-SSS-cys also improved coronary flow and left ventricular developed pressure. This evidence highlights cysSSH as an important pre-conditioning molecule for protecting against myocardial IRI. (33)

1.4.3 Cardiovascular endothelium and NO pathways

Nitric oxide (NO) plays a vital role in the maintenance of endothelial function and cardiovascular homeostasis, (18) but following endothelial dysfunction, numerous studies have revealed that NO is impaired (35) and attributes to myocardial IRI. (36) One potential mechanism that has been described to contribute towards endothelial dysfunction is eNOS uncoupling, which leads to reduced NO levels during myocardial ischaemia-reperfusion, as mentioned previously. (36) The major causation of eNOS uncoupling is the oxidant/antioxidant imbalance seen in oxidative stress. Uncoupled eNOS are converted to superoxide anion, adding further imbalance in favour of the oxidants, accelerating the effects of oxidative stress such as atherogenesis and lipid peroxidation. (36) When tetrahydrobiopterin (BH4) is limited, eNOS becomes uncoupled. Two molecules of BH4 bind to each eNOS dimer, promoting L-arginine oxidation. (37) A study by Cai et al showed that BH4 helps to improve endothelial function and preserve eNOS dimerisation, highlighting that increasing BH4 levels may be an efficacious therapy for the maintenance of eNOS function. (38)

1.5 PKG 1α oxidation and the heart

1.5.1 PKG 1α physiology and functions

Protein kinase cGMP dependent 1α (PKG 1α) is an enzyme isoform encoded by the PKG 1 gene on chromosome 10, and along with PKG 1β and PKG 2 is a key mediator in the NO-sGC-cGMP pathway (figure 1.4). (39) PKG 1α is most prevalent in smooth muscle cells, platelets, and purkinje cells. (39) Smooth muscle cells are especially important as seen in an ALDH2 study by Zhao et al, which showed that PASMCs are the main site of action for the ALDH2 enzyme to carry out its cardioprotective functions. The presence of PKG 1α will help to protect and preserve these smooth muscle cells for ALDH2, highlighting a symbiotic relationship between the two enzymes. (40) After IRI, ALDH2 limits damage to endothelial cells, through its ability to detoxify 4-HNE. (41)

A 2020 study by Chan et al, found that a mutation in the PKG 1 gene led to thoracic aortic aneurysms and dissections. This substitution mutation of arginine to glutamine disrupted the binding of the enzyme to cGMP. (42) PKG 1α plays a key role in the regulation and coordination of the heartbeat. Cardiomyocyte shortening and lengthening seen in systole and diastole is caused by the movement of calcium in and out of the cell. PKG 1α influences this movement and consequently cardiomyocyte length. If oxidation of PKG 1α is inhibited, the cycle of calcium in the cardiomyocytes is disrupted, leading to an altered cardiac cycle. (43)

1.5.2 PKG 1α oxidation

An earlier study by Prysyazhna et al also highlights the enzyme's importance in cardioprotection, as they found that a single atom change in the enzyme's structure resulted

in the loss of vasodilatory action, leading to hypertension. (44) NO and prostacyclin are key mediators of vasodilation, however, inhibition of their production leads to significant vasorelaxation. This vasorelaxation is known as endothelium-derived hyperpolarizing factor (EDHF) and is imperative for the control of blood pressure. Hydrogen peroxide is a major part of EDHF and gives rise to a disulfide bond between the two α subunits of PKG 1α, which causes activation of the kinase independent from the NO-sGC-cGMP pathway. (45) To test the importance of PKG 1α oxidation with EDHF and blood pressure control, a knock-in (KI) mouse with 'redox dead' PKG 1α was studied, and found to block the actions of hydrogen peroxide in EDHF, negating any vasorelaxation, and increasing resistance levels and hypertension. These studies highlight and emphasise the benefits of PKG 1α oxidation. (44)

In contrast, a 2015 study by Nakamura et al, opposes this stance. (46) It is recognised in this study as mentioned previously that PKG 1α can be oxidised to form a disulfide bond between homodimer subunits at cysteine 42, initiating a shift of the 75 kilodaltons (kDa) monomer band to 150kDa, leading to vasorelaxation. However, its overall impact on cardiovascular homeostasis remains to be fully elucidated. The study revealed that PKG 1α oxidation contributes to abnormal heart remodelling following a period of pressure overload. In addition, the 'redox dead' PKG 1α genotype tested by Prysyazhna et al, (44) was also tested in this study by Nakamura et al. (46) The study by Prysyazhna et al found that 'redox dead' PKG 1α increased hypertension, however, Nakamura et al found that the 'redox dead' enzyme group showed better adaptation to cardiac stress. (44)(46) The study by Nakamura et al took this argument further, hypothesising that reduced PKG 1α may be the most beneficial form of the enzyme to maximise its cardioprotective properties. This is because reduced PKG 1α is

translocated to the outer plasma membrane, which enhances the suppression of transient receptor potential channel 6 (TRPC6), in turn boosting anti-hypertrophic signalling. The authors concluded that these results show that PKG 1α oxidation prevents a positive reaction to stress, which provides reasoning for the variation of opinion between academics regarding the efficacy of PKG 1α pathway stimulation in heart disease. (46)

1.6 Summary

The devastating effects of AMI are well documented and widely known, however, the prevalence of this disease remains high and novel therapeutic interventions are warranted to prevent myocardial injury and prevent the onset of heart failure. Therefore, it is extremely important to continue to investigate the pathophysiology of myocardial IRI. Particularly the role of persulfides and enzymes such as PKG 1α and ALDH2, as they may show potential for future treatments. However current knowledge of persulfides and their association with PKG 1α oxidation and ALDH2 is limited. Recently, persulfide donor, cys-SSS-cys has been shown to be cardioprotective against myocardial IRI by reducing infarct size in C57BL/6 mice, (33) however mechanism(s) remain to be determined. Thus, this project will focus on elucidating the mechanism by which cys-SSS-cys protects against myocardial injury and whether this is mediated via PKG 1α oxidation (e.g dimerization at the cys42 residue) when ALDH2 is deficient.

1.7 Hypothesis

Hypothesis 1: ALDH2 deficiency leads to an increase in infarct size and PKG 1α dimerisation following myocardial ischaemia-reperfusion injury.

Hypothesis 2: cys-SSS-cys elicits cardioprotective effects through a decrease in infarct size following ischaemia-reperfusion injury.

1.8 Aims

1. Investigate the effects of ALDH2 deficiency on infarct size by using an ex vivo myocardial ischaemia-reperfusion injury model.
2. Determine the effect of ALDH2 deficiency on PKG 1α dimerisation following myocardial ischaemia-reperfusion injury.
3. Establish whether cys-SSS-cys protects against myocardial injury when ALDH2 is deficient.

2. Materials and methods

Treatment conditions

Age-matched ALDH2 wild-type (WT) and knock-out (KO) mice (20-25g) were maintained in-house. All of the experiments and protocols carried out in the present study were conducted in accordance with the specifications of the 1986 United Kingdom Animals (Scientific Procedures) Act and were approved by the Animal Welfare and Ethical Review Body.

Materials

Unless otherwise mentioned reagents were purchased from Sigma/VWR.

2.1 Genotyping of ALDH2 mice

DNA extraction

Mouse ear clippings were obtained from the Biomedical services unit, University of Birmingham, for genotyping and were processed using Bioline ISOLATE II Genomic DNA Kit manufacturer guidelines (Bioline; London, UK). Briefly, the first step in the DNA extraction was Pre-lysis, where 180 µL of lysis buffer GL and 25 µL proteinase K solution was added to an Eppendorf containing the ear clipping, ensuring that the sample was completely covered with solution and vortexed. Incubation at 56°C took place for 2 hours until the sample was lysed. The sample was further lysed by vortexing briefly and adding 200 µL Lysis Buffer G3. The samples were then vortexed again and incubated at 70°C for 10 minutes. The DNA binding conditions were adjusted by vortexing the sample briefly and adding 210 µL ethanol (96-100%) before vortexing again vigorously. The DNA was bound by placing ISOLATE II Genomic DNA Spin Column in a 2 ml Collection Tube, where the sample was loaded into the column and centrifuged for 1 minute at 11,000 x g, flow through was discarded. The silica membrane was washed by adding 500 µL Wash Buffer GW1, then by centrifuging for 1 minute at 11,000 x g, flow through was discarded. This was followed by addition of 600 µL of Wash Buffer GW2, then centrifuging again for 1 minute at 11,000 x g, flow through was discarded. The silica membrane was dried by centrifuging for 1 minute at 11,000 x g, to remove residual ethanol. Then the spin column was placed in a 1.5 ml microcentrifuge tube. The DNA was eluted by adding 100 µl preheated Elution Buffer G (70°C) onto the centre of

the silica membrane. This was followed by incubation at room temperature for 1 minute and centrifuging for 1 minute at 11,000 x g, the flow through was collected this time.

ALDH2 DNA electrophoresis

To prepare the DNA mixture for polymerase chain reaction (PCR), 18.5µl (per sample) of the reaction mixture was used, which was made up of 10µl 2 x Red MyTaq Mix, 6µl autoclaved sterile water, 1µl 10µM ALDH2 Int 3, 1µl 10µM ALDH2 F1 (forward primer), and 0.5µl of 10µM ALDH2 R3 (reverse primer). These primers were all sourced from Sigma Aldrich Life Sciences. The mastermix was vortexed, then 18.5µl, and 1µl of the DNA sample were added into each Eppendorf tube. Positive controls were used, this included ALDH2 DNA that have been run successfully before and the negative control with master mix and just water. The samples were placed into the PCR machine and run on the following cycles as depicted in Figure 2.1.

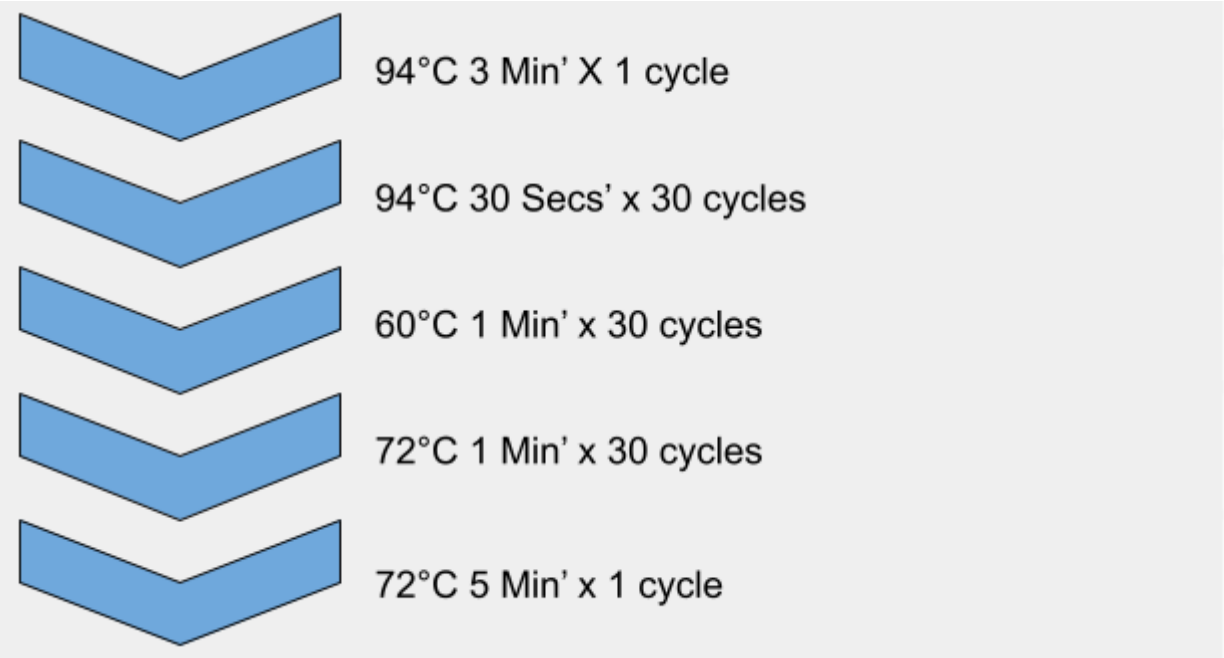

Figure 2.1. *PCR cycles for ALDH2 DNA electrophoresis.*

While PCR took place the agarose gel was made. Firstly, two rubber ends were placed on the plates and tape was added to each of the ends, to create a tight seal. A 2% agarose gel was made with 2g agarose (Abnova) in 100ml 1 x TAE (Sigma), before being placed in the microwave for 1 minute 40 seconds. 5µl sybr safe (Thermofisher) was added to the agarose mixture, which was swirled to mix. The agarose mixture was poured onto the plate, a comb was added to create wells, and after ensuring there are no air bubbles, was left for 30 minutes to set. After 30 minutes, it was placed into the tank, and 1 x TAE was poured over, covering the gel.

Once PCR was complete 15µl of the samples (including positive and negative controls) and 5µl of the DNA ladder (Promega) were loaded into their respective well. After putting on the lid and connecting to the power pack the gels were run at 100 volts (V) for 40 minutes. After gel electrophoresis, the DNA bands for homozygous ALDH2 WT (597 base pairs (bp)) and homozygous ALDH2 KO (280bp) were detected by using a ChemiDoc MP imaging system. An example of ALDH2 genotype bands is shown in figure 2.2.

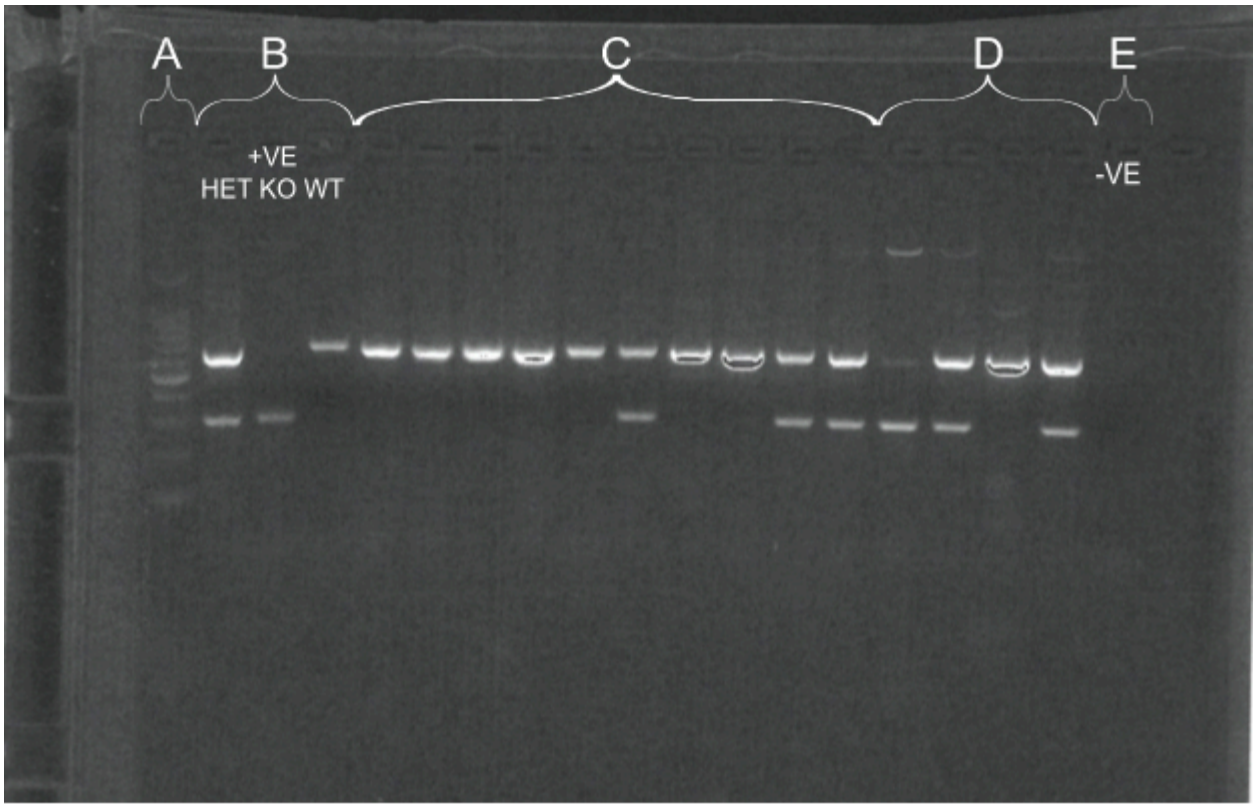

Figure 2.2. *ALDH2 genotyping with controls. (A) Lane 1 shows the DNA ladder, used as a reference to be able to accurately estimate and compare genotypes of ALDH2 mice. (B) Lanes 2-4 are the positive controls. Lane 2 has 2 bands showing that it is the heterozygous (HET) genotype positive control. Lane 3 is the knockout (KO) mouse positive control as only the lower 280bp band is present, and lane 4 is the wild-type (WT) mouse positive control as only the top 597bp band is present. (C) Lanes 5-14 are litter 0096, which has 7 homozygous samples and 3 heterozygous samples. (D) Lanes 15-18 are litter 0097, which has 3 heterozygous samples and one homozygous sample. (E) Lane 19 has no visible bands, as it is the negative control that was loaded with water only.*

2.2 Langendorff protocol

Langendorff is a well-established model to assess the direct effect of different enzymes such as ALDH2 and the effect of IRI on the heart. (47) Briefly, the ALDH2 WT or KO mouse was anaesthetised by administering an intraperitoneal injection of sodium pentobarbitone (200mg/kg) mixed 50:50 with the anticoagulant heparin (1000 IU/kg). Pedal reflex was then checked to ensure that the mouse was anaesthetised. To isolate the heart, the diaphragm was exposed by a transabdominal incision and then cut to expose the thoracic cavity. The thorax

was opened by a bilateral incision along the lower margin of the last to first ribs and the thoracic cage was opened, exposing the heart. The heart was lifted slightly before incision of the aorta, vena cava and pulmonary vessels. The heart was then immersed immediately in ice-cold Krebs-Henseleit buffer (KHB), of which a 5-litre stock solution was made up (see table 2.1). The heart was cleaned and the aorta was cannulated with a blunt-ended 21 gauge needle, before the isolated heart was retrogradely perfused with fresh 37°C, gassed (95% O_2 and 5% CO_2) KHB, at a continuous pressure of 80mmHg. This was carried out with the STH pump controller (ADInstruments), which can control the flow of biological liquids by altering the flow rate signal sent to a peristaltic pump. (48) The heart sample was monitored and kept at 37°C and paced at 600 beats per minute (bpm) using the 6002 simulator (Harvard apparatus). The hearts were then subjected to 40 minutes of stabilisation, 30 minutes of global ischaemia, and then 2 hours of reperfusion. (49) For analysis of the effects of cys-SSS-cys on infarct size, hearts were perfused for 10 minutes at the onset of reperfusion with either vehicle control (KHB) or 100μM cys-SSS-cys (33). After 2 hours of reperfusion the hearts were stained with 2,3,5-Triphenyltetrazolium chloride (TTC; Sigma) for infarct analysis (section 2.2.1) or snap frozen for the assessment of PKG 1a dimerization (section 2.3).

Table 2.1. *Ingredients of Krebs-Henseleit buffer used for Langendorff heart model.*

Chemical	Concentration mM	5L	Source
Nacl	118.5	34.63g	Sigma
KCL	25	10.5g	VWR
Kh2po4	4.7	1.77g	VWR
Nahco3	1.2	1.47g	Thermo fisher
Mgso4	1.2	0.8g	VWR
Glucose	11	9.9g	Thermo fisher
Cacl2	1.4	1.04g	VWR

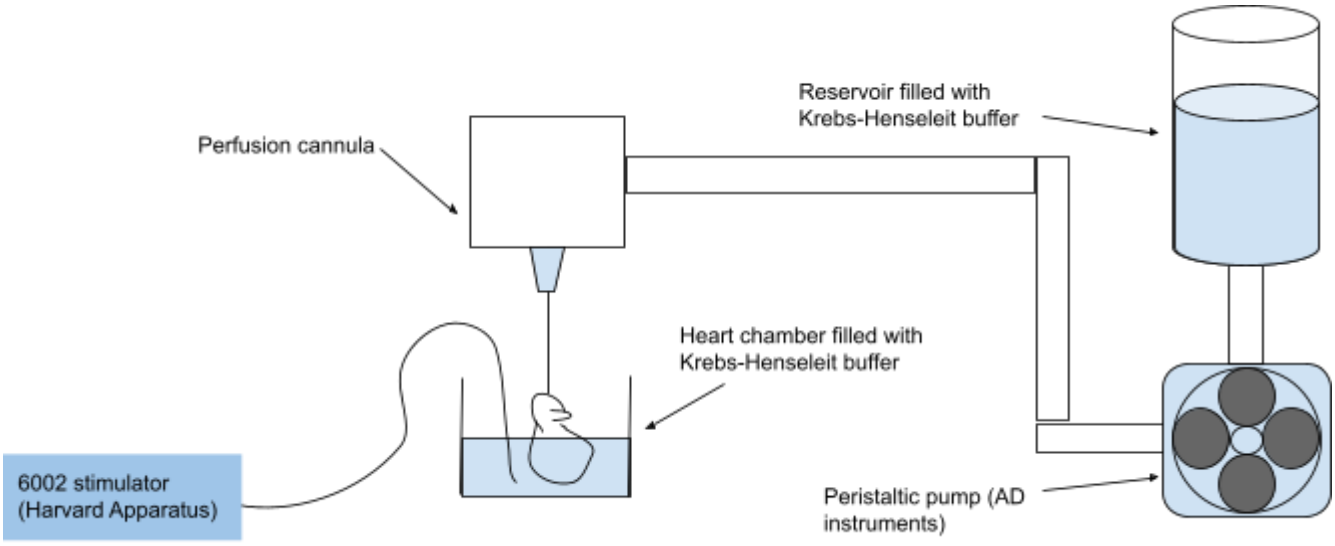

Figure 2.3. *Langendorff protocol. Suspension of the heart in Krebs-Henseleit buffer, with fresh buffer being stored in the reservoir for perfusion through the 21 gauge needle. There is a 6002 stimulator for pacing the heart at 600 bpm, and a peristaltic pump for perfusion of the fresh Krebs-Henseleit buffer.*

2.2.1 Assessment of infarct size

TTC staining for mouse hearts

As previously described, (33) a 1% TTC solution (0.5g/50ml phosphate-buffered saline (PBS); Sigma) was made fresh on the day of the Langendorff protocol and incubated at 37°C, until required. At the end of the 2 hours of reperfusion, 5ml of the 1% TTC solution was carefully perfused into the heart. The heart was then placed into 5ml of the 1% TTC and incubated at 37°C for further 10 minutes. After 10 minutes the heart was blotted, and stored in an Eppendorf tube at -20°C.

Preparation of heart slices

A thin layer of 5% agarose (5g agarose in 100ml of distilled water; abnova) mixture was poured into trays and allowed to set before removing the hearts from the freezer and adding cold 2.5% glutaraldehyde (Sigma) for 2 minutes. The hearts were placed onto the trays with 5% agarose and held in place with a needle. Additional 5% agarose was then poured over to cover the hearts while making sure the agarose is not boiling hot. After the agarose set, the hearts were sliced from base to apex of the heart into 700μM sections by a vibratome (Campden instruments). After sectioning, each slice was placed into its own well within the 12-well plate, followed by adding 1ml of 10% formaldehyde (38% formaldehyde stock solution; Sigma) diluted 50ml/200ml in double distilled water (ddH_2O) to each heart section. The slices were left overnight in the 10% formaldehyde at room temperature. 24 hours later the formaldehyde was removed and replaced with PBS. The slices were incubated for a further 24 hours at 4°C. The next day, the sections were compressed between perspex plates, 0.57mm apart, and scanned using photoshop (Adobe version 2021).

Using Image J (National Institutes of Health) the photoshop images were traced by adjusting the brightness and drawing around the infarct of each heart to determine their size. The contrast was enhanced between the dead tissue (infarcted area) and the rest of the heart to allow tracing. After measuring the area of the whole heart and the area of the infarct, the percentage infarct was calculated for each slice. An average was calculated for percentage infarct for the slices of each heart sample, to compare ALDH2 WT and KO hearts.

2.3 Western blotting for PKG 1α oxidation

2.3.1 Dimerization protocol for PKG 1α oxidation

Heart samples were collected from storage at -80°C in liquid nitrogen to ensure that the samples are kept under frozen conditions at all times. The samples were weighed and immediately placed back into the liquid nitrogen. Under liquid nitrogen conditions, the hearts were crushed using a pestle and mortar to create a 10% (weight/volume) homogenate using a homogenisation buffer (50ml of ice-cold 100mM Tris-HCL buffer was added to 100mM maleimide and 1 tablet of protease inhibitor). The homogenate was quickly pipetted into an Eppendorf tube to prevent oxidation of the samples, placed back into the liquid nitrogen to snap freeze, and then allowed to thaw on ice. This freeze thaw cycle was carried out twice. The homogenate was diluted 1:5, using a 2 x sample buffer (100mM Tris-HCL, 4% SDS, 0.2% bromophenol blue, 20% glycerol, and 0.048g maleimide) to create the Western blotting samples.

2.3.2 Western blotting

SDS polyacrylamide gel electrophoresis

To run the samples for Western blotting, SDS-PAGE was carried out, using an 8% gel. An 8% gel was used because the proteins being targeted are 75 and 150 kilodaltons (kDa), see table 2.2. Two different polyacrylamide gels were made up, the resolving gel, and the stacking gel. The resolving gel (8%) was made up of 2.67ml 30% acrylamide, 3.38ml deionised water, 3.8ml 1M Tris-HCL ph 8.8, 100µl SDS, 10µl tetramethylethylenediamine (TEMED), and 100µl ammonium sulfate (APS), see table 2.3. APS was added last to trigger the polymerization

reaction. The resolving gel was poured between the two plates of glass, with a 2cm gap left at the top. This was overlaid with butan-1-ol (Sigma), to remove any air bubbles. Polymerization took approximately 30 minutes, during which the stacking gel was made up. This consisted of 0.9ml 30% acrylamide, 4ml deionised water, 720µl 1M Tris-HCL ph6.8, 60µl SDS, 10µl TEMED, and 100µl APS, see table 2.4. Excess water was poured off along with the butan-1-ol before the addition of APS to the stacking gel, as again polymerization occurred immediately. The stacking gel was poured onto the surface of the resolving gel to the top of the glass plate, before the insertion of the comb to form 1ml sample wells. Polymerization took around 20 minutes, then once the stacking gel had set the gels were stored in the fridge overnight.

Table 2.2. *Percentage acrylamide gel for different ranges of separation, allowing for the targeting of specific proteins. In this study, an 8% acrylamide gel was run for the detection of 75kDa and 150kDa proteins.*

Acrylamide %	Range of separation (kDa)
15	12-45
12.5	10-70
10	15-100
8	25-200
5	57-212

Table 2.3. *The resolving gel is made up of each component at the 8% level due to the size of the proteins of interest.*

	8%
30% Acrylamide	2.67ml
Deionised water	3.38ml
1M Tris-HCL ph 8.8	3.8ml
SDS (from 10% stock solution)	100µl
TEMED	10µl
APS	100µl

Table 2.4. *The stacking gel was made up of the same components as the resolving gel, apart from 1M Tris-HCL with a pH level of 6.8 as opposed to 8.8. The volume of each component was fixed, independent of the % level the gels were run at.*

	Stacking gel
30% Acrylamide	0.9ml
Deionised water	4ml
1M Tris-HCL ph 6.8	720µl
SDS (from 10% stock solution)	60µl
TEMED	10µl
APS	100µl

The next day, the gel plates were assembled in the tank, with the ladders facing each other. Then the running buffer was added to the tank, which was made with 100ml of 10% running buffer stock and 10ml of 10% SDS (Scientific Laboratory Supplies) before being made up to 1L with ddH_2O. The running buffer stock consisted of 30g Tris base and 144g Glycine, which was made to 1L with ddH_2O. Before loading, samples were centrifuged for 10 minutes at 14,000 rpm at room temperature. After the combs were removed, a precision plus protein dual colour standards ladder (biorad) was used, of which 5µl was pipetted into well 1 of the gel. This is also to determine the molecular weight of the proteins. Then 10µl of each sample was pipetted into their well using Western blotting tips. Once the samples were loaded the lid was attached and the electrodes were connected to the power pack, making sure to connect the right colour electrode to the right colour terminal (black to black, red to red). The gels were run at 150V for approximately 1 hour, or until the samples had run down the gel. During this time the wet transfer to the polyvinylidene difluride (PVDF; VWR) membrane was prepared.

Wet transfer method

Firstly, the transfer buffer was made up which contained 6g Tris base, 28.8g glycine, and 400 ml methanol. It was then made up to 2L with ddH_2O and stored at 4°C to improve heat dissipation. The PVDF membrane was placed in a container to soak in methanol for 30 minutes, then transfer buffer until required, and four sheets of blotting paper and four fibre pads were soaked in the transfer buffer, before being stored at 4°C.

After the gel had run, the glass plates containing the gel were separated using a scraper, before the gel was equilibrated in a transfer buffer. The gel was prepped for transfer in a sandwich-like structure. Firstly, the cassette was placed down, open with the grey side down on a clean surface. The fibre pad was then placed on top, followed by one sheet of blotting paper pre-soaked in the transfer buffer. After this, the gel was placed on top, in the opposite orientation to that which the gel was loaded. This is so that the PVDF membrane reads in the same orientation as the gel. The PVDF membrane was placed onto the gel, followed by the second blotting paper and fibre pad. Each layer was rolled over gently to remove any air bubbles. The cassette was closed, locked into place, and positioned in the electrode module in the buffer tank. An ice pack was added to the tank to keep conditions cold before the transfer buffer was added to the blotting mark. A stirrer bar was added to maintain consistent buffer temperature and ion distribution across the tank. The transfer was run at 100V for 1.5 hours on the magnetic stirrer.

Antibody exposure and ECL detection

Following wet transfer, the membrane was placed in 5% blotting-grade blocker milk, and placed on a shaker for 1 hour, to minimise background interference on the results. After blocking, the milk was poured off and the primary antibody, PKG 1α (Enzo)-1:1000-5%-milk was added. The container was placed on a shaker in a cold room overnight. The next day, the primary antibody was removed, and the membrane was washed with PBS. The blots were washed for 1 hour again on a shaker at room temperature, with the PBS being changed every 15 minutes. After 1 hour the PBS was poured off and the secondary antibody, anti-rabbit (cell-signalling)-1:1000-1%-BSA was added. The blot was placed back on the shaker for an hour at room temperature, before being washed again for 1 hour post incubation of the secondary antibody, with the PBS being changed every 15 minutes like before. The ECL reagent (Fisher Scientific) was made up by mixing reagents A and B in a 15ml tube. The membranes were then placed in the ECL reagent and onto a shaker for 3 minutes. Excess ECL reagent was blotted onto a tissue, and the membranes were placed into a plastic wallet in the developing cassette. The cassette was taken to the dark room, where an X-ray film was added for the transfer. The membrane and X-ray film were exposed for various lengths of time (e.g. 15 seconds, 30 seconds, 1 minute, and 2 minutes). After the films have developed the blots were rinsed with PBS to remove the ECL.

The above steps were repeated for the addition of the loading control, to validate whether the samples were equally loaded. The blots were placed in bovine serum albumin (BSA) at 1g/20ml and left on a shaker for 1 hour. Sodium azide was made, 1g/10ml ddH_20 (10% azide). Of this 100µl was added to 20ml of BSA, which gave a concentration of 0.05% azide in 5%

BSA. After 1 hour of blocking with these concentrations the membrane was quickly washed twice with PBS. The primary antibody was added and the blots were incubated overnight on a shaker in the cold room at 4°C. The next day the primary antibody, GAPDH-(Abcam)-1:1000-5%-BSA was removed and the blots were washed with PBS for 1 hour, changing the PBS every 15 minutes. Then the secondary antibody, anti-rabbit (cell-signalling)-1:1000-1%-BSA was added, and the container was left on the shaker for 1 hour. Washing took place again for 1 hour with new PBS every 15 minutes. The blots were placed in the ECL reagent and onto a shaker for 3 minutes, before being placed in the developing cassette. The dark room was used again to transfer to X-ray film, exposing the membrane and X-ray film for 5 minutes before being run in the developer.

2.3.3 Analysis of blots

The western blot for each set was analysed by measuring expression at 75kDa (monomer) and 150kDa (dimer) bands. Each dimer and monomer value was measured in photoshop using the rectangle tool to calculate the mean in each well. These values were then used to calculate the percentage dimerisation for each heart sample.

2.4 Statistical analysis

All data are presented as means ± standard error of the mean (SEM). N is the number of heart samples used. Statistical analysis was carried out with GraphPad Prism software (version 9) using a one-way ANOVA for comparisons between multiple groups. A P value of ≤ 0.05 was considered significant.

3. Results

3.1 Cysteine trisulfide reduces infarct size following IRI in ALDH2 deficient mice

First, we assessed the effect of cysSSH donor, cys-SSS-cys (100 μM), on infarct size in ALDH2 WT and KO hearts following myocardial ischaemia-reperfusion. As depicted in figure 3.1, increased infarct size was observed in both ALDH2 WT and KO control groups, respectively. One-way ANOVA followed by Bonferroni's test revealed that there was no significant difference in infarct size between the WT control group when compared to the KO control group (51.98% *vs* 44.24%; respectively; p=0.4959; N=5-9). Furthermore, whilst cys-SSS-cys attenuated infarct size in both ALDH2 WT and KO mouse hearts, statistical analysis showed that there was no significant difference between the WT cys-SSS-cys group and the KO cys-SSS-cys group (22.54% *vs* 26.11%; respectively, p=0.9011; N=7 per group).

However, when comparing the WT control group with hearts treated with 100uM cys-SSS-cys, we observed a significant reduction in percentage infarct size in the WT mice (51.98% *vs* 22.54%, respectively; p<0.0001; N=7-9). A similar trend was also observed with ALDH2 KO mice, whereby there was a significant attenuation in myocardial injury in cys-SSS-cys treated ALDH2 KO when compared with the ALDH2 WT control group (51.98% *vs* 26.11%, respectively; p=0.0001; N=7-9). Furthermore, compared to the KO control group, treatment with cys-SSS-cys significantly reduced infarct size in both WT and KO mice; (WT 44.24% *vs* 22.54%, respectively; p=0.0044; N=5-7) (KO 44.24% *vs* 26.11%, respectively; p=0.0195; N=5-7).

A

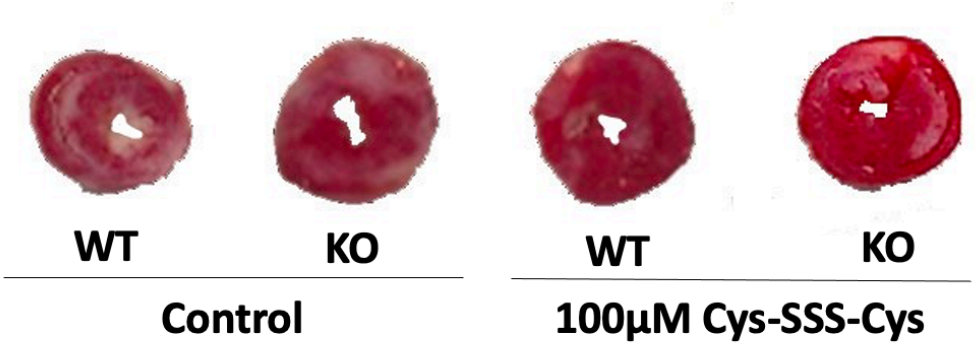
WT
KO
WT
KO
Control
100µM Cys-SSS-Cys

B

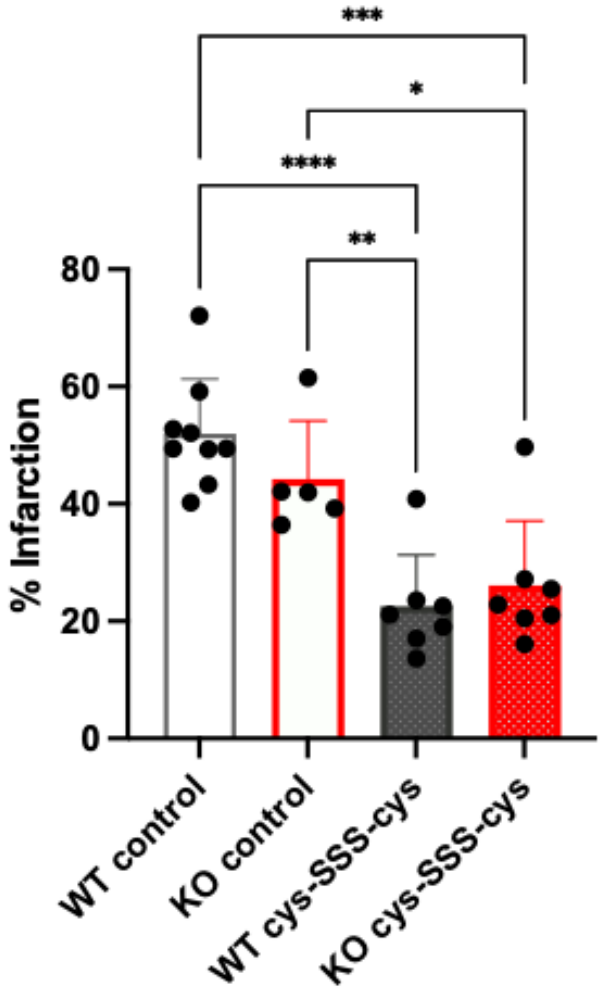
***
*
****
**
80
60
40
20
0
% Infarction
WT control
KO control
WT cys-SSS-cys
KO cys-SSS-cys

Figure 3.1. (A) *Representative images of ALDH2 infarct sizes of wild type (WT) and knockout (KO) vehicle control and WT and KO cys-SSS-cys (100 μM) groups. Heart slices were stained with 2,3,5-Triphenyltetrazolium chloride (TTC), red staining indicates viable tissue and white areas indicate non-viable (necrotic) tissue.* ***(B)*** *Percentage infarct of WT control, KO control, WT cys-SSS-cys (100 μM), and KO cys-SSS-cys (100 μM) groups. Data displayed as mean ± SEM; *P ≤ 0.05, **P ≤ 0.01, ***P ≤ 0.001, and ****P ≤ 0.0001 as determined by one-way ANOVA with Bonferroni's test, n=5-9 per group.*

3.2 Increased PKG 1α oxidation in ALDH2 deficient mice following myocardial IRI

As part of our overall investigation of ALDH2, we studied the effects of ALDH2 deficiency on PKG 1α dimerisation, following ischaemia-reperfusion.

As shown in figure 3.2, a comparison of both basal groups showed that there was no significant difference in PKG 1α dimerisation in the WT basal group versus the KO basal group (26.93% *vs* 26.84%, respectively; p>0.9999; N=6 per group). In contrast, increased PKG 1α dimerisation was observed in both ALDH2 WT and KO mouse hearts when subjected to 30 minutes of ischaemia and 2 hours of reperfusion. However, there was no significant difference between the ALDH2 WT 2 hours reperfusion group versus the KO 2 hours reperfusion control group (41.17% *vs* 52.89%, respectively; p=0.0737; N=6-7).

PKG 1α dimerisation significantly increased in the KO 2 hours reperfusion group when compared to the WT basal group (26.93% *vs* 52.89%; p<0.0001; N=6 per group) and the KO basal group (26.84% *vs* 52.89%; p<0.0001; N=6 per group). The WT 2 hours reperfusion group also showed a significant increase in percentage dimerisation when compared to the WT basal group (26.93% *vs* 41.17%; p=0.0227; N=6-7) and the KO basal group (26.84% *vs* 41.17%; p=0.0218; N=6-7).

A

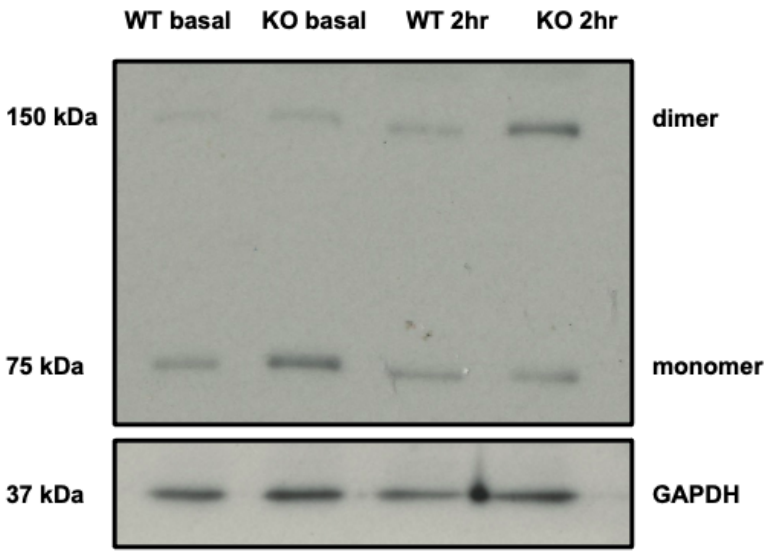
WT basal
KO basal
WT 2hr
KO 2hr
150 kDa
dimer
75 kDa
monomer
37 kDa
GAPDH

B

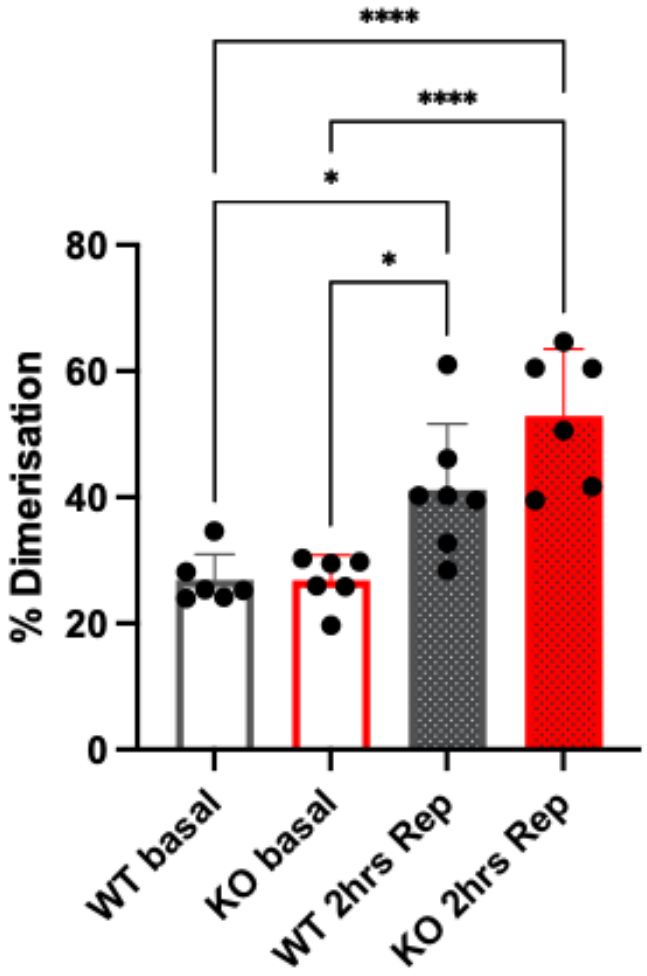
****
****
*
*
% Dimerisation
80
60
40
20
0
WT basal
KO basal
WT 2hrs Rep
KO 2hrs Rep

Figure 3.2. (A) *PKG 1α representative blot showing the 150kDa dimer bands and 75kDa monomer bands for WT basal, KO basal, WT 2 hours reperfusion, and KO 2 hours reperfusion. The GAPDH loading control is also included which is shown at 37kDa.* ***(B)*** *Percentage dimerisation of WT basal, KO basal, WT 2 hours reperfusion, and KO 2 hours reperfusion groups. Data displayed are means ± SEM; *P ≤ 0.05, **P ≤ 0.01, ***P ≤ 0.001, ****P ≤ 0.0001 as determined by one-way ANOVA with Bonferroni's test, n=6-7 per group.*

4. Discussion

4.1 Elucidation of the role and mechanism of cysteine trisulfide in protection against IRI

Current knowledge of mitochondrial enzyme ALDH2 and its association with cysSSH following myocardial IRI is limited. ALDH2 is known to protect against oxidative stress, and the cysSSH donor, cysSSScys, has been shown to reduce toxic aldehyde lipid peroxidation products 4 HNE and MDA. (45) However, further investigation is necessary to improve our knowledge of these molecules and to identify them as potential future treatment options. Therefore, this study investigated the effects of ALDH2 deficiency and cys-SSS-cys on infarct size. We carried out this study through analysis of the heart infarct images using Image J, showing that cys-SSS-cys decreases infarct size.

Results showed that 10 minutes of perfusion with cys-SSS-cys (100μM) in both WT and KO mice significantly reduced infarction size when compared to both WT and KO control groups. The most significant reduction in infarct size was in the WT cys-SSS-cys group when compared to the WT control group (51.98% *vs* 22.54%, respectively; $p<0.0001$; N=7-9). These results mean however that we cannot state with confidence that ALDH2 deficiency lead to increased infarct sizes independently, and so we accept the null hypothesis for ALDH2

deficiency. We can however state that cys-SSS-cys decreased infarct size and we can reject the null hypothesis for cys-SSS-cys.

These results emphasise the importance of cys-SSS-cys for cardiovascular health. While ALDH2 deficient groups did not show a significant increase in infarct size, the WT cys-SSS-cys group had the lowest mean percentage infarction (22.54%), supporting our hypothesis that ALDH2 deficiency leads to an increase in infarct size, at least in combination with cys-SSS-cys. On the other hand, the WT control group had a greater mean percentage infarction (51.98%) compared to the KO control group (44.24%), which suggests alternatively that ALDH2 deficiency leads to a decrease in infarct size, again at least in the absence of cys-SSS-cys. Further investigation may prove valuable in being able to state with more confidence the effect of ALDH2 on infarct size, as well as other cardioprotective measurements, and gain a better understanding of its relationship with cys-SSS-cys. The results may suggest that there may be a symbiotic relationship between ALDH2 and cys-SSS-cys, with their combination in the WT cys-SSS-cys group presenting the most efficacious result.

Previous studies have also highlighted persulfides as key cardioprotective molecules, with the potential for them to be used as pre-conditioning agents for myocardial IRI. (45) In the present study we demonstrate that cys-SSS-cys reduces infarction size, but in addition to this, we know from wider research that its effects also include reduced lipid peroxidation, and as a result reduced cell membrane damage of cardiomyocytes. (33) cysSSH concentration has been shown previously to increase after myocardial ischaemia. (33) This is believed to be due

to reduced cysteine dioxygenase activity, which oxidises cysteine to cysteine sulfinic acid during normoxia. (50) As well as this there is reduced activity of sulfide-quinone oxidoreductase which breaks down H_2S. (51) A study by Stubbert et al, (52) found that another mechanism that hydropersulfides like cysSSH are involved in is the activation of PKG 1α oxidation, which we know helps mediate vasorelaxation as well as the cardiac cycle. (45) With this knowledge another topic to investigate in the future could be the effects of cys-SSS-cys on PKG 1α oxidation, to see if there is a direct link between the two.

Like persulfides, ALDH2 is also supported by previous studies as a cardioprotective enzyme. (53)(54) One similar study to ours by Ma et al also investigated the effects of ALDH2 deficiency using WT and KO mice following ischaemia-reperfusion. They also included an ALDH2 overexpressing genotype in their investigation. They found that overexpression led to a significant decrease in infarction, and infarction size in the KO group was significantly bigger. This result was the same for recovery of post-ischaemic left ventricular function, as well as hypoxia/reoxygenation-induced cardiomyocyte contractile dysfunction. Another study outcome was that ALDH2 reduced 4-HNE levels after an increase due to ischaemia-reperfusion. (53) These cardioprotective effects may occur through an AMPK-dependent induction of autophagy taking place throughout ischaemia, followed by Akt-dependent reduction of autophagy throughout reperfusion. The regulation of the AMPK and Akt pathway is believed to be regulated through liver kinase B1 (LKB1) and phosphate and tensin homolog (PTEN) signalling. (53) This study highlights the importance of the AMPK-Akt-Mtor pathway which may be of interest for further investigation for the mitigation of IRI through autophagy regulation. These findings were seconded by Guo et al, (54) who also

found that ALDH2 decreases 4-HNE levels. As well as this they identified ALDH2 deficiency in stroke-prone spontaneously hypertensive rats (SHR-SP). Another interesting study outcome was that ALDH2 knockout rats did not show any neuroprotective effects of the enzyme protein kinase C epsilon type (PKCε). (54) PKCε also has an important protective role in the cardiovascular system, through modulation of the contractile function of the myocardial sarcomere, (55) and metabolic function of myocardial mitochondria. (56)(57)

One limitation of this study would be the small sample size. There were 9 WT control samples, 7 WT cys-SSS-cys and KO cys-SSS-cys samples, and only 5 KO control samples. A greater sample size would help validate our results and provide a more accurate statistical analysis.

Future research opportunities may include investigating what the optimal intrinsic conditions are for cysSSH production. Cysteinyl-tRNA synthetase (CARS) enzymes are also able to produce cysSSH endogenously. (58) Investigation of what chemical conditions trigger this enzymatic release of cysSSH may help improve our knowledge of this mechanism for the potential treatment of cardiovascular diseases. This could be to do with the redox status of the microenvironment (the balance of oxidants vs antioxidants). In addition, a comparison of CARS enzymes and the cysSSH donor cys-SSS-cys may be valuable to see whether there is a significant difference between the efficacy of these production/donation pathways for the mitigation of IRI.

In the 2023 study by Griffiths et al, (33) it was found that increased levels of cysSSH led to a reduction in lipid peroxidation and the formation of reactive aldehydes, resulting in improved myocardial recovery. (33) However this link has not been proven to be a direct correlation, so further investigation of this mechanism in heart tissue is necessary to gain a better understanding of their interaction. A hypothetical mechanism has been proposed (figure 4.1), but investigation of these reactions is necessary to identify any interaction with new unknown molecules. (33)

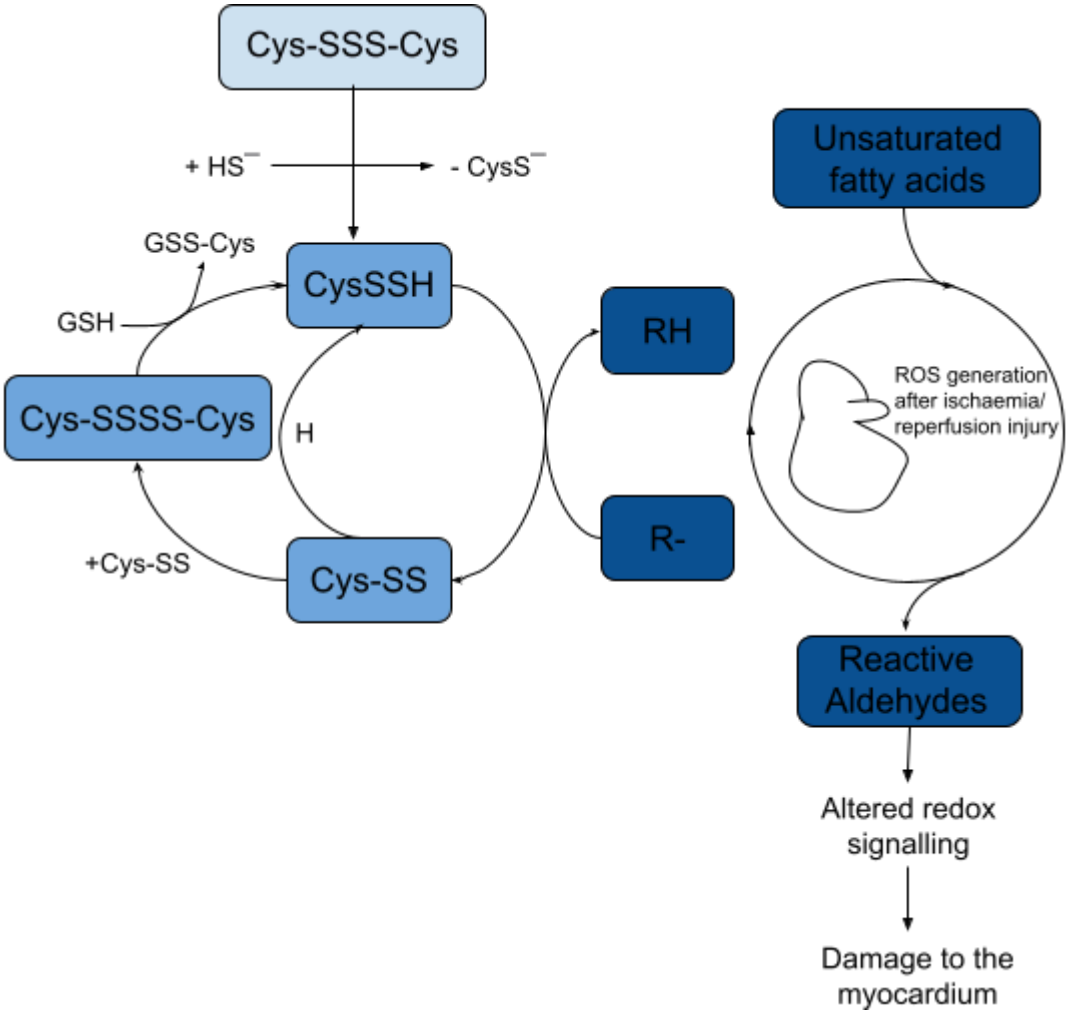

Figure 4.1. *Proposed mechanism of how increased cysSSH reduces lipid peroxidation and its effects - adapted from Griffiths et al (2023). (33)*

It may also be beneficial to investigate cysSSH levels following a longer period of reperfusion, to see if its concentration continued to decrease. As well as this, the optimal dosage of exogenous cardioprotective agents like cys-SSS-cys should be investigated further, as a lower dose (10μM) reduced levels of 4-HNE (μg/ml) in heart tissue compared to a higher dose (100μM) which had no effect compared to the control. To complicate our understanding, levels of the other main product of lipid peroxidation MDA were only found to decrease after the higher 100μM dose of cys-SSS-cys, with no change being observed with the lower 10μM dose. (33) This could be attributed to the unique nature of hydropersulfides which have both oxidant and antioxidant characteristics. (59)

Although ALDH2 deficiency did not lead to a significant decrease in infarct size as expected, it would be beneficial to investigate the effects of an ALDH2 overexpressing type, as seen in the study by Ma et al. (53) This ALDH2 overexpressing type was investigated in a recent 2023 study by Pan et al, (60) where analysis of infarction size also took place after utilising the Langendorff perfusion model, (47) before mice hearts were subjected to 30 minutes ischaemia followed by 90 minutes reperfusion. ALDH2 overexpression was induced via intracardiac delivery, which led to reduced infarct size as well as increased contractile function. This overexpression improved the detoxification of 4-HNE, presenting ALDH2 as an effective pre-conditioning agent for the mitigation of IRI. (60) These findings highlight the potential of further investigation of ALDH2 overexpression, and whether there may be a difference in efficacy when the delivery method is altered like in the study described above.

4.2 The role of ALDH2 in PKG 1α oxidation and its efficacy for protection against IRI

Results showed that 2 hours of reperfusion in WT and KO groups significantly increased percentage PKG 1α dimerisation compared to WT and KO basal groups with no reperfusion. The most significant increase in percentage PKG 1α dimerisation was in the KO 2 hours reperfusion group. Although we previously highlighted a potential symbiotic relationship between ALDH2 and PKG 1α, this study showed that ALDH2 deficiency does not increase PKG 1α dimerisation. These results mean that we cannot state with confidence that ALDH2 deficiency lead to increased PKG 1α dimerisation independently and we therefore accept the null hypothesis. However, we can state that 2 hours of reperfusion did lead to increased PKG 1α dimerisation.

As described previously, hydropersulfide levels decrease during reperfusion, (33) and are also involved in the activation of PKG 1α oxidation, (52) so their uptake may provide a potential biological explanation for their decrease in concentration during 2 hours of reperfusion. With the KO 2 hours reperfusion group having the largest percentage PKG 1α dimerisation, the results suggest that ALDH2 deficiency increases PKG dimerisation. While statistical analysis showed us that this result was not significant, WT 2 hours reperfusion vs KO 2 hours reperfusion returned the closest p-value (0.0737) to the significance value (0.05) of all the insignificant statistical comparisons.

Previous studies argue for and against the activation of PKG 1α oxidation as it seems to have both desirable and unwanted effects on the cardiovascular system. (44-46) A recent study by Prysyazhna et al (61) outlines the structure of PKG1α and its role in the cardiovascular

system. PKG 1α contains three domains; leucine zipper, regulatory and catalytic (figure 4.2). In the leucine zipper, a disulfide bridge can form between cysteine 42 (C42) of two PKG 1α proteins. It is also responsible for basal dimerisation and interaction with G-kinase anchoring proteins (GKAP). In the regulatory domain, C117 and C195 can bind together. Also, there are two binding sites for cGMP, one high affinity and one low affinity. In the catalytic domain, C312 and C518 can bind together. PKG1α's affinity for cGMP is more than ten times greater than PKG1β. This study highlights PKG1α oxidation as a vital reaction for cardiovascular homeostasis. (61) Supporting this, PKG1α oxidation decreases vascular smooth muscle cell calcium (Ca2+), contributing to vasodilation, (62) and C42 binding effects EDHF-dependent lowering of blood pressure. (63)

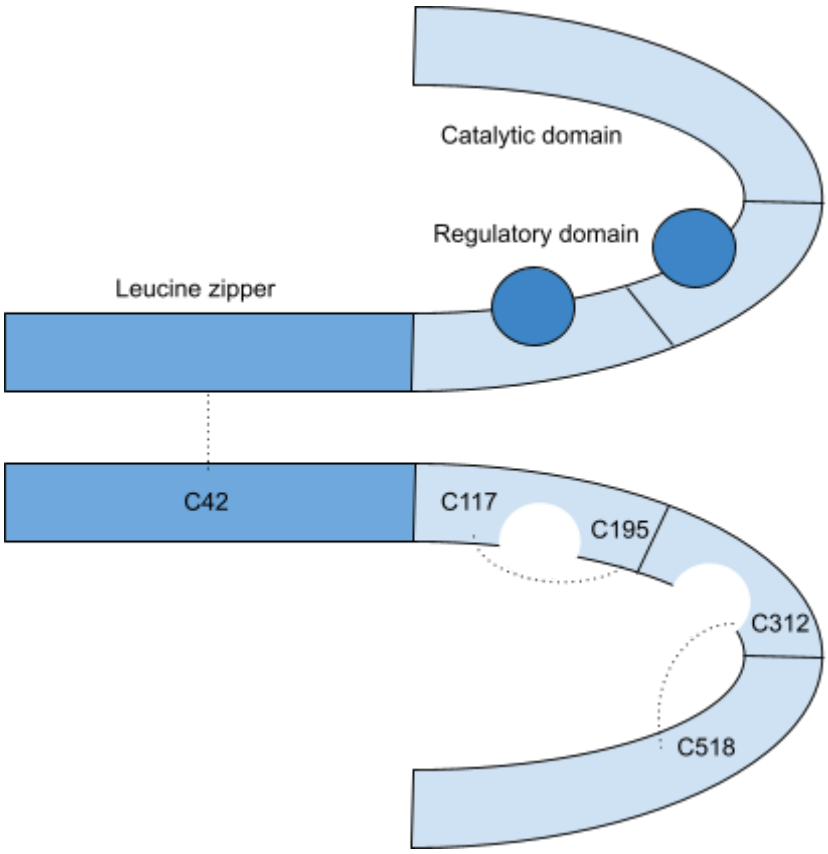

Figure 4.2. *The three domains of PKG 1α, and each pair of cysteines that can bind to form a disulfide bridge. C42-C42, C117-C195, and C312-C518. Adapted from Prysyazhna et al (2015). (62)*

While PKG 1α oxidation has been emphasised as a vital reaction in cardiovascular homeostasis, (62) the 2015 study by Nakamura et al provides an opposing stance. (46) Specifically, one of the results of this study was that dimerisation at C42 worsens the heart's response to pressure overload. Additionally, during myocardial recovery there was no reduction in levels of oxidative stress, with the ratio of oxidised glutathione to lipid peroxidation products (MDA and 4-HNE) equal in both WT and KI mice. They also found that PKG 1α oxidation limits its ability to phosphorylate TRPC6, and that reduced PKG 1α was more effective at blocking this pathway. TRPC6 is responsible for triggering calcineurin/nuclear factor of activated T cells (Cn/NFAT) signalling, a pathological signalling cascade. (46)

Small sample size was a limitation of this study as well. There were 7 samples for the WT 2 hours reperfusion group and only 6 for the KO 2 hours reperfusion group, as well as the WT and KO basal groups. A greater sample size would help validate our results and provide more accurate statistical analysis. Variability may have had a big effect on the outcome of this study. As mentioned, a comparison of the WT 2 hours reperfusion group and the KO 2 hours reperfusion group returned a p-value of 0.0737, which is very close to the significance value of 0.05. Repetition of this study with more samples may help us to compare these groups again with more accuracy and determine whether ALDH2 deficiency significantly increases PKG 1α dimerisation.

The decrease in hydropersulfide levels during reperfusion may be in part due to their role in the activation of PKG 1α oxidation, (52) however, this should be investigated further to outline how they carry out this role. Looking forward similarly to our first study, the cysSSH donor

cys-SSS-cys could be investigated, to see what effect it has on PKG 1α dimerisation. Depending on the outcome, it may help us to determine the efficacy of PKG 1α dimerisation for the mitigation of IRI.

Continued investigation of PKG1α oxidation and infarct size is warranted, as well as other parameters of myocardial recovery measured in previous persulfide studies such as left ventricular developed pressure and coronary flow. (33)

4.3 Summary

Overall, our results indicate that ALDH2 deficiency does not increase infarct size or PKG 1α dimerisation, however, we have demonstrated that cys-SSS-cys does decrease infarct size, improving our understanding of the role of hydropersulfides in cardiovascular disease. We also identified that 2 hours of reperfusion increases PKG 1α dimerisation, although whether PKG 1α oxidation is good or bad for the cardiovascular system and protection against IRI remains to be fully recognised, with recent studies supporting both arguments. (44-46) PKG 1α oxidation should be investigated further through combination with proven cardioprotective agents such as cysSSH, to help develop our understanding and uncover its effects. The cardioprotective effects of cys-SSS-cys that have been highlighted in this study should be investigated further alongside other hydropersulfide species to identify optimal dosage and intrinsic conditions for its therapeutic application.

5. References

(1) Ritchie H, Spooner F, Roser M. Causes of death [Internet]. Our World in Data. 2018 [cited 2023Jan25]. Available from: https://ourworldindata.org/causes-of-death#what-do-people-die-from

(2) Innes JA. Davidson's Essentials of Medicine. Edinburgh: Elsevier; 2020.

(3) Coronary artery disease [Internet]. Mayo Clinic. Mayo Foundation for Medical Education and Research; 2022 [cited 2023Feb10]. Available from: https://www.mayoclinic.org/diseases-conditions/coronary-artery-disease/diagnosis-treatment/drc-20350619

(4) What are the signs and symptoms of coronary heart disease? [Internet]. What Are the Signs and Symptoms of Coronary Heart Disease? - NHLBI, NIH. 2014 [cited 2023Jan25]. Available from: https://web.archive.org/web/20150224034615/http://www.nhlbi.nih.gov/health/health-topics/topics/cad/signs

(5) Morrow DA. Myocardial infarction: A companion to braunwald's heart disease. St. Louis, MO: Elsevier; 2017.

(6) Steg PG, James SK, Atar D, Badano LP, Lundqvist CB, Borger MA, et al. ESC guidelines for the management of acute myocardial infarction in patients presenting with st-segment elevation. European Heart Journal. 2012;33(20):2569–619.

(7) O'Connor RE, Brady W, Brooks SC, Diercks D, Egan J, Ghaemmaghami C, et al. Part 10: Acute coronary syndromes. Circulation. 2010;122(18_suppl_3).

(8) Fitridge R, Thompson MM. Mechanisms of vascular disease: A reference book for Vascular Specialists. Adelaide: The University of Adelaide Press; 2011.

(9) Marnett LJ. Lipid peroxidation—DNA damage by Malondialdehyde. Mutation Research/Fundamental and Molecular Mechanisms of Mutagenesis. 1999;424(1-2):83–95.

(10) González-Minero FJ, Bravo-Díaz L, Ayala-Gómez A. Rosmarinus officinalis L. (rosemary): An ancient plant with uses in personal healthcare and cosmetics. Cosmetics. 2020;7(4):77.

(11) National Center for Biotechnology Information [Internet]. ALDH2 aldehyde dehydrogenase 2 family member [Homo sapiens (human)] - Gene - NCBI; [cited 2023 Apr 1]. Available from: https://www.ncbi.nlm.nih.gov/gene/217

(12) Ohta Shigeo, Ohsawa Ikuroh, Kamino Kouzin, Ando Fujiko, Shimokata Hiroshi. Mitochondrial ALDH2 deficiency as an oxidative stress. Annals of the New York Academy of Sciences. 2004;1011(1):36–44.

(13) Chen C-H, Ferreira JC, Mochly-Rosen D. ALDH2 and cardiovascular disease. Aldehyde Dehydrogenases. 2019;:53–67.

(14) Guo H, Yu X, Liu Y, Paik DT, Justesen JM, Chandy M, et al. SGLT2 inhibitor ameliorates endothelial dysfunction associated with the common *aldh2* alcohol flushing variant. Science Translational Medicine. 2023;15(680).

(15) Sun L, Ferreira JC, Mochly-Rosen D. ALDH2 activator inhibits increased myocardial infarction injury by nitroglycerin tolerance. Science Translational Medicine. 2011;3(107).

(16) Cao R, Fang D, Wang J, Yu Y, Ye H, Kang P, et al. ALDH2 overexpression alleviates high glucose-induced cardiotoxicity by inhibiting NLRP3 inflammasome activation. Journal of Diabetes Research. 2019;2019:1–11.

(17) Zhang Y, Ren J. Autophagy in ALDH2-elicited cardioprotection against ischemic heart disease: Slayer or savior? Autophagy. 2010;6(8):1212–3.

(18) NASEEM K. The role of nitric oxide in cardiovascular diseases. Molecular Aspects of Medicine. 2005;26(1-2):33–65.
(19) Altaany Z, Yang G, Wang R. Crosstalk between hydrogen sulfide and nitric oxide in endothelial cells. Journal of Cellular and Molecular Medicine. 2013;17(7):879–88.
(20) Griffiths K, Lee JJ, Frenneaux MP, Feelisch M, Madhani M. Nitrite and myocardial ischaemia reperfusion injury. where are we now? Pharmacology & Therapeutics. 2021;223:107819.
(21) Domínguez R, Maté-Muñoz J, Cuenca E, García-Fernández P, Mata-Ordoñez F, Lozano-Estevan M et al. Effects of beetroot juice supplementation on intermittent high-intensity exercise efforts. Journal of the International Society of Sports Nutrition. 2018;15(1).
(22) Domínguez R, Cuenca E, Maté-Muñoz J, García-Fernández P, Serra-Paya N, Estevan M et al. Effects of Beetroot Juice Supplementation on Cardiorespiratory Endurance in Athletes. A Systematic Review. Nutrients. 2017;9(1):43.
(23) Nyakayiru J, Jonvik K, Trommelen J, Pinckaers P, Senden J, van Loon L et al. Beetroot Juice Supplementation Improves High-Intensity Intermittent Type Exercise Performance in Trained Soccer Players. Nutrients. 2017;9(3):314.
(24) Lundberg JO, Weitzberg E, Gladwin MT. The nitrate–nitrite–nitric oxide pathway in physiology and therapeutics. Nature Reviews Drug Discovery. 2008;7(2):156–67.
(25) Kuypers MM, Marchant HK, Kartal B. The microbial nitrogen-cycling network. Nature Reviews Microbiology. 2018;16(5):263–76.
(26) Lundberg JO, Govoni M. Inorganic nitrate is a possible source for systemic generation of nitric oxide. Free Radical Biology and Medicine. 2004;37(3):395–400.
(27) Cyclic GMP. [cited 2023Mar15]. Available from: https://www.reading.ac.uk/nitricoxide/intro/no/cgmp.htm
(28) Köken T, İnal M. The effect of nitric oxide on ischemia–reperfusion injury in Rat liver. Clinica Chimica Acta. 1999;288(1-2):55–62.
(29) Khanna A, Cowled PA, Fitridge RA. Nitric oxide and skeletal muscle reperfusion injury: Current Controversies (Research Review). Journal of Surgical Research. 2005;128(1):98–107.
(30) Cowled PA, Khanna A, Laws PE, Field JBF, Varelias A, Fitridge RA. Statins inhibit neutrophil infiltration in skeletal muscle reperfusion injury. Journal of Surgical Research. 2007;141(2):267–76.
(31) Nitric oxide and its role in lipid peroxidation - Violi - 1999 ... [Internet]. [cited 2023Jan30]. Available from: https://onlinelibrary.wiley.com/doi/10.1002/%28SICI%291520-7560%28199907/08%2915%3A4%3C283%3A%3AAID-DMRR42%3E3.0.CO%3B2-U
(32) Barayeu U, Schilling D, Eid M, Xavier da Silva TN, Schlicker L, Mitreska N, et al. Hydropersulfides inhibit lipid peroxidation and ferroptosis by scavenging radicals. Nature Chemical Biology. 2022;19(1):28–37.
(33) Griffiths K, Ida T, Morita M, Lamb RJ, Lee JJ, Frenneaux MP, et al. Cysteine hydropersulfide reduces lipid peroxidation and protects against myocardial ischaemia-reperfusion injury - are endogenous persulfides mediators of ischaemic preconditioning? Redox Biology. 2023;60:102605.
(34) Bonetti PO, Lerman LO, Lerman A. Endothelial dysfunction. Arteriosclerosis, Thrombosis, and Vascular Biology. 2003;23(2):168–75.

(35) Mudau M, Genis A, Lochner A, Strijdom H. Endothelial dysfunction : The early predictor of atherosclerosis. Cardiovascular Journal of Africa. 2012;23(4):222–31.
(36) Łuczak A, Madej M, Kasprzyk A, Doroszko A. Role of the enos uncoupling and the nitric oxide metabolic pathway in the pathogenesis of autoimmune rheumatic diseases. Oxidative Medicine and Cellular Longevity. 2020;2020:1–15.
(37) Yang Y-M, Huang A, Kaley G, Sun D. Enos uncoupling and endothelial dysfunction in aged vessels. American Journal of Physiology-Heart and Circulatory Physiology. 2009;297(5).
(38) Cai S, Khoo J, Mussa S, Alp NJ, Channon KM. Endothelial nitric oxide synthase dysfunction in diabetic mice: Importance of tetrahydrobiopterin in Enos dimerisation. Diabetologia. 2005;48(9):1933–40.
(39) PRKG1 protein kinase cgmp-dependent 1 [homo sapiens (human)] - gene - NCBI [Internet]. National Center for Biotechnology Information. U.S. National Library of Medicine; [cited 2023Feb14]. Available from: https://www.ncbi.nlm.nih.gov/gene/5592
(40) Zhao Y, Wang B, Zhang J, He D, Zhang Q, Pan C, et al. ALDH2 (aldehyde dehydrogenase 2) protects against hypoxia-induced pulmonary hypertension. Arteriosclerosis, Thrombosis, and Vascular Biology. 2019;39(11):2303–19.
(41) Lee H-L, Hee S-W, Hsuan C-F, Yang W, Huang J-Y, Lin Y-L, et al. A novel ALDH2 activator ad-9308 improves diastolic and systolic myocardial functions in streptozotocin-induced diabetic mice. Antioxidants. 2021;10(3):450.
(42) Chan MH, Aminzai S, Hu T, Taran A, Li S, Kim C, et al. A substitution in cgmp-dependent protein kinase 1 associated with aortic disease induces an active conformation in the absence of cgmp. Journal of Biological Chemistry. 2020;295(30):10394–405.
(43) Understanding how oxidation of a protein called PKGI-alpha regulates the Heartbeat [Internet]. BHF. [cited 2023Feb15]. Available from: https://www.bhf.org.uk/research-projects/modulation-of-cardiac-systolic-and-diastolic-properties-by-oxidation-dependant-activation-of-protein
(44) Prysyazhna O, Rudyk O, Eaton P. Single atom substitution in mouse protein kinase G eliminates oxidant sensing to cause hypertension. Nature Medicine. 2012;18(2):286–90.
(45) Feelisch M, Akaike T, Griffiths K, Ida T, Prysyazhna O, Goodwin JJ, et al. Long-lasting blood pressure lowering effects of nitrite are no-independent and mediated by hydrogen peroxide, persulfides, and oxidation of protein kinase G1A redox signalling. Cardiovascular Research. 2019;116(1):51–62.
(46) Nakamura T, Ranek MJ, Lee DI, Shalkey Hahn V, Kim C, Eaton P, et al. Prevention of pkg1α oxidation augments cardioprotection in the stressed heart. Journal of Clinical Investigation. 2015;125(6):2468–72.
(47) Sutherland FJ, Shattock MJ, Baker KE, Hearse DJ. Mouse isolated perfused heart: Characteristics and cautions. Clinical and Experimental Pharmacology and Physiology. 2003;30(11):867–78.
(48) STH Pump Controller [Internet]. ADInstruments. [cited 2023Feb27]. Available from: https://www.adinstruments.com/products/sth-pump-controller
(49) Madhani M, Hall AR, Cuello F, Charles RL, Burgoyne JR, Fuller W, et al. Phospholemman ser69 phosphorylation contributes to sildenafil-induced cardioprotection against reperfusion injury. American Journal of Physiology-Heart and Circulatory Physiology. 2010;299(3).

(50) Stipanuk MH. Metabolism of sulfur-containing amino acids: How the body copes with excess methionine, cysteine, and sulfide. The Journal of Nutrition. 2020;150.
(51) Landry AP, Ballou DP, Banerjee R. Hydrogen sulfide oxidation by sulfide quinone oxidoreductase. ChemBioChem. 2020;22(6):949–60.
(52) Stubbert D, Prysyazhna O, Rudyk O, Scotcher J, Burgoyne JR, Eaton P. Protein kinase G iα oxidation paradoxically underlies blood pressure lowering by the reductant hydrogen sulfide. Hypertension. 2014;64(6):1344–51.
(53) Ma H, Guo R, Yu L, Zhang Y, Ren J. Aldehyde dehydrogenase 2 (ALDH2) rescues myocardial ischaemia/reperfusion injury: Role of Autophagy Paradox and toxic aldehyde. European Heart Journal. 2010;32(8):1025–38.
(54) Guo J-M, Liu A-J, Zang P, Dong W-Z, Ying L, Wang W, et al. ALDH2 protects against stroke by clearing 4-hne. Cell Research. 2013;23(7):915–30.
(55) Huang X, Walker JW. Myofilament anchoring of protein kinase C-epsilon in cardiac myocytes. Journal of Cell Science. 2004;117(10):1971–8.
(56) Baines CP, Song C-X, Zheng Y-T, Wang G-W, Zhang J, Wang O-L, et al. Protein kinase cε interacts with and inhibits the permeability transition pore in cardiac mitochondria. Circulation Research. 2003;92(8):873–80.
(57) Ping P, Zhang J, Pierce WM, Bolli R. Functional proteomic analysis of protein kinase C ε signalling complexes in the normal heart and during Cardioprotection. Circulation Research. 2001;88(1):59–62.
(58) Kolluru GK, Shen X, Kevil CG. Reactive sulfur species. Arteriosclerosis, Thrombosis, and Vascular Biology. 2020;40(4):874–84.
(59) Switzer CH, Fukuto JM. The antioxidant and oxidant properties of hydropersulfides (RSSH) and polysulfide species. Redox Biology. 2022;57:102486.
(60) Pan G, Roy B, Harding P, Lanigan T, Hilgarth R, Thandavarayan RA, et al. Effects of intracardiac delivery of aldehyde dehydrogenase 2 gene in myocardial salvage. Gene Therapy. 2022;30(1-2):115–21.
(61) Prysyazhna O, Eaton P. Redox regulation of cgmp-dependent protein kinase iα in the cardiovascular system. Frontiers in Pharmacology. 2015;6.
(62) Müller PM, Gnügge R, Dhayade S, Thunemann M, Krippeit-Drews P, Drews G, et al. H2O2 lowers the cytosolic ca2+ concentration via activation of cgmp-dependent protein kinase iα. Free Radical Biology and Medicine. 2012;53(8):1574–83.
(63) Shimokawa H. 2014 Williams Harvey Lecture: Importance of coronary vasomotion abnormalities--from bench to bedside. European Heart Journal. 2014;35(45):3180–93.